

A Comparison of Landsat-8 OLI, Sentinel-2 MSI and PlanetScope Satellite Imagery for Assessing Coastline Change in El-Alamein, Egypt [†]

Kamal Darwish ^{1,*}  and Scot Smith ²¹ Department of Geography, Faculty of Arts, Minia University, El Minia 61519, Egypt² School of Forest, Fisheries & Geomatics Sciences, University of Florida, Gainesville, FL 32611, USA;

sesmith@ufl.edu

* Correspondence: kamal.srogy@mu.edu.eg; Tel.: +2-010-9356-6658

[†] Presented at the 8th International Electronic Conference on Sensors and Applications, 1–15 November 2021; Available online: <https://ecsa-8.sciforum.net>.

Abstract: The objective of this study was to provide an assessment of coastline extraction and change analysis using different sensors from three satellites over time. Imagery from Landsat-8 OLI, Sentinel-2A MSI, and PlanetScope-3B were used to detect geomorphological changes along the El-Alamein coastline on the Mediterranean Sea between August 2016 and August 2021. The normalized difference water index (NDWI) was applied to automate, detect and map water bodies based on thresholding techniques and coastline extraction. The extracted coastlines were analyzed using geographic information systems (GIS)-based digital shoreline analysis system (DSAS.v5) model, a GIS software tool for the estimation of shoreline change rates calculated through two statistical techniques: net shoreline movement (NSM) and end point rate (EPR). The results indicate that measuring coastline morphological change using satellite-based imagery depends very much on the resolution of the imagery. It is necessary to tailor the selection of imagery to the accuracy of the measurement needed. Higher resolution imagery such as PlanetScope (3 m) produces higher resolution measurements. However, medium resolution imagery from Landsat may be sufficiently good for objectives requiring less spatial resolution.

Keywords: Coastline Change Delineation; Landsat 8; Sentinel-2; PlanetScope; Alamein coast; satellite remote sensing; DSAS; GIS

check for
updates

Citation: Darwish, K.; Smith, S. A Comparison of Landsat-8 OLI, Sentinel-2 MSI and PlanetScope Satellite Imagery for Assessing Coastline Change in El-Alamein, Egypt. *Eng. Proc.* **2021**, *10*, 23. <https://doi.org/10.3390/ecsa-8-11258>

Academic Editor: Stefano Mariani

Published: 1 November 2021

Publisher's Note: MDPI stays neutral with regard to jurisdictional claims in published maps and institutional affiliations.



Copyright: © 2021 by the authors. Licensee MDPI, Basel, Switzerland. This article is an open access article distributed under the terms and conditions of the Creative Commons Attribution (CC BY) license (<https://creativecommons.org/licenses/by/4.0/>).

1. Introduction and Literature Review

Coastlines are one of the most morphologically dynamic landforms on Earth and change in a short period [1]. Coastline morphological changes are one of the major environmental problems affecting densely populated areas around the world. Studies of coastline change is very important for coastal planning and management. About 80% of the world's coasts are changing at rates ranging from 1 cm/year to 10 m/year [2]. Coastline changes under the influence of natural and anthropogenic factors [3].

Satellite remote sensing imagery has become essential for monitoring coastal change due to large coverage, frequency and low cost [4]. Different types of imagery can be obtained from satellite remote sensing such as hyperspectral, multispectral, and radar. In this study, multispectral satellite imagery was used to detect coastline changes because it has several advantages, including a large number of data records, frequency at different times and total Earth coverage [3]. The availability of the time series of optical remote sensing images can be used effectively for water body monitoring and coastline extraction for change analysis over time to help understand the influence of the natural factors and human activities on coastal change [5]. Water body mapping using spectral indices have been used for coastline detection and extraction using Landsat satellite imagery for nearly

50 years because of their availability, reliability and low cost [6]. In 2013, Landsat 8 was launched, and its operational land imager (OLI) sensor providing multispectral images (11 spectral bands) at a 30 m instantaneous field of view and 16-day revisit time. Sentinel-2A was launched in 2015 with a multispectral scanner capable of acquiring data in 13 spectral bands between, with a revisit time of 5-days [7]. Landsat-8 and Sentinel-2A provide reliable results for water body mapping and change monitoring [8,9]. Planet Inc. operates PlanetScope, RapidEye and SkySat. Planet sells processed data in a variety of formats to serve different uses [10]. Imagery has four spectral bands captured as a single red–green–blue (RGB) scene. The PlanetScope satellite is a CubeSat 3U form factor ($10 \times 10 \times 30$ cm). Planet operates over 130 satellites capable of imaging the entire land/water surface of the Earth every day. Planet offers three levels of PlanetScope imagery: (1) basic scene product (level 1B), (2) an ortho-scene product (level 3B) and (3) an ortho-tile product (level 3A) [11]. The ortho-rectified surface reflectance PlanetScope data is critical in many environmental applications.

The extraction of water bodies and coastline change detection using Landsat-based remote sensing are used by many researchers [3,6,12,13]. The same is true for Sentinel-2 [14] and PlanetScope imagery [15,16]. Studies have been conducted comparing Landsat 8, Sentinel-2, and PlanetScope imagery for coastline changes [17], water quality assessment [18], bathymetry mapping [17] and other combined use [19]. In Egypt, several studies have been conducted to study coastal change. Studies assessing shoreline morphodynamics using remote sensing conducted by Frihy and Deabes [20] used Landsat imagery taken between 1988 and 2011 to assess shoreline changes. Studies by Emam and Soliman [21,22] analyzed shoreline changes along Marina El-Alamein Resort based on Landsat TM, ETM+ and OLI taken between 1987 and 2017. Awad and El-Sayed [23] analyzed changes of the El-Omayed coast between 1984 and 2018 using Landsat imagery and were used to predicate shoreline change to the year 2050.

The main objective of this study was to compare the application of Landsat, Sentinel and Planet imagery for assessing coastline change along the El-Alamein coast in Egypt. The study performed spatial computation of the coastline change rate using GIS and the digital shoreline analysis system (DSAS).

2. Materials and Methods

2.1. Study Area

The study area is located along the Mediterranean coast of Egypt, approximately 100 km west of Alexandria city (Figure 1). It played a critical role during World War II in a major battle between the Allied troops and the Germans. Winning that battle is credited with turning the tide against Germany. There are memorial sites and cemeteries commemorating the thousands of men who died in that terrible battle. Today, armed and viable landmines are still found along the coast and inland, despite the fact El-Alamein is becoming an important holiday villa site. El-Alamein is a beautiful setting and so plays a major role in Egypt's future.

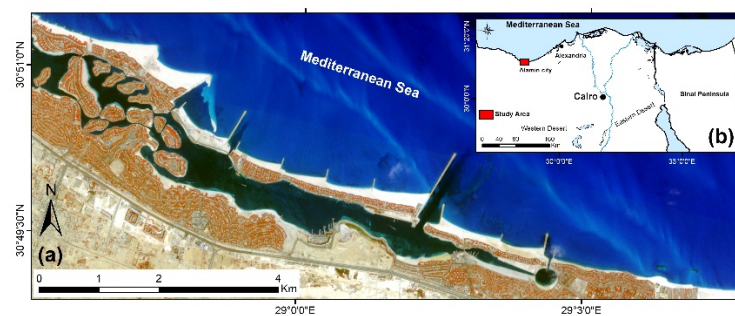


Figure 1. Study area. (a) Study area (image from PlanetScope taken in 2021). (b) Location of study area in northern Egypt.

2.2. Materials

Landsat-8 operational land-imager (OLI) images were acquired between 2016 and 2021 at an interval of five years. They were downloaded in GeoTIFF format from the United States Geological Survey (USGS) Earth Explorer Website (<http://earthexplorer.usgs.gov/> (12 October 2021)) as shown in Table 1. These Landsat datasets constitute the useable database of “good quality, level 2 product”. They were radiometrically corrected to surface reflectance. Sentinel-2 multispectral instrument (MSI) level-1C images taken between 2016 and 2021 were download from the European Space Agency website. Sentinel-2 are at the top of atmosphere reflectance. PlanetScope images taken between 2016 and 2021 were collected for the study area, as shown in Figure 1. The images were atmospherically corrected to surface reflectance using the 6S v2.1 radiative transfer code. The PlanetScope Lab also did radiometric correction using sensor telemetry and a sensor model [18].

Table 1. Specifications of satellite imagery used in this study.

Year	Acquired Date	Satellite/Sensor ¹	Path/Row	IFOV (m)
2016	08/25/2016	Landsat-8/OLI	178/39	30
	08/20/2016	Sentinel-2A/MSI	L1C_T35RPQ	10
	08/12/2016	PlanetScope/3B	075305	3
2021	08/07/2021	Landsat-8/OLI	178/39	30
	08/14/2021	Sentinel-2A/MSI	L1C_T35RPQ	10
	08/28/2021	PlanetScope/3B	082015	3

¹ Landsat downloaded from USGS Website: <https://earthexplorer.usgs.gov/> (13 October 2021), Sentinel-2A downloaded from <https://scihub.copernicus.eu/dhus/#/home> (10 October 2021), PlanetScope downloaded from <https://www.planet.com> (15 October 2021).

2.3. Methods

The methods of this study are divided into three stages: (1) remote sensing data collection and pre-processing procedures, including: band combination, geometrical and radiometric corrections; (2) applied NDWI/MNDWI indices for automatic coastline extraction as shown in Figure 2; and (3) GIS-based spatial analysis of coastline changes using the digital shoreline analysis system (DSAS). DSAS calculates gaps amongst the coastline positions during defined periods (Figure 3). Two statistical parameters were used to assess coastline change detection: firstly, net shoreline movement (NSM), which is the total movement between the two-shoreline positions, and secondly, end point rate (EPR), which was calculated by dividing the distance of shoreline movement by the time elapsed between the two shorelines, as shown in equation 1. The rate is reported in meters per year with positive values indicating accretion and negative values indicating erosion. Normalized difference water index (NDWI)/modified normalized difference water index (MNDWI) water indices applied for study area using ERDAS Imagine algorithms to detect the water/land feature by a thresholding method using ENVI 5.3 software for coastline detection, NDWI was proposed by McFeeters (1996) for water resource assessment. An NIR band and a green band were used to enhance discrepancies between surface water and non-water features [24]. McFeeters’s NDWI is calculated in Equation (2) as:

$$\text{EPR (m/year)} = \frac{\text{Shoreline movement from A to B (m)}}{\text{Years duration from A to B (years)}} \quad (1)$$

$$\text{NDWI} = \frac{(\text{Band}_{\text{Green}} - \text{Band}_{\text{NIR}})}{(\text{Band}_{\text{Green}} + \text{Band}_{\text{NIR}})} \quad (2)$$

where $\text{Band}_{\text{Green}}$ is the reflectance value of the green band and Band_{NIR} reflection value of the NIR band. The derived new index is called MNDWI [25], which is expressed in Equation (3) as:

$$\text{MNDWI} = \frac{\text{Band}_{\text{Green}} - \text{Band}_{\text{MIR}}}{\text{Band}_{\text{Green}} + \text{Band}_{\text{MIR}}} \quad (3)$$

where $Band_{MIR}$ is the reflectance of the MIR band. The index NDWI were applied on PlanetScope (4 bands) and Sentionel-2A imagery, while Landsat-8 applied MNDWI.

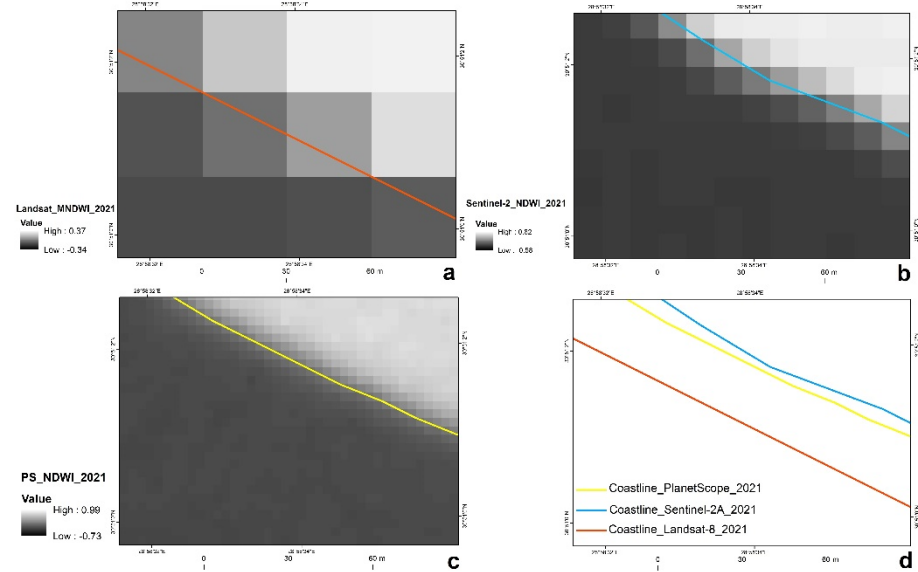


Figure 2. Coastline feature extraction. Sub-figure (a) Landsat-8 MNDWI image August 2021; sub-figure (b) Sentinel-2A NDWI image August 2021; sub-figure (c) PlanetScope NDWI image August 2021; and sub-figure (d) spatial displacement between coastlines at the same time, August 2021.

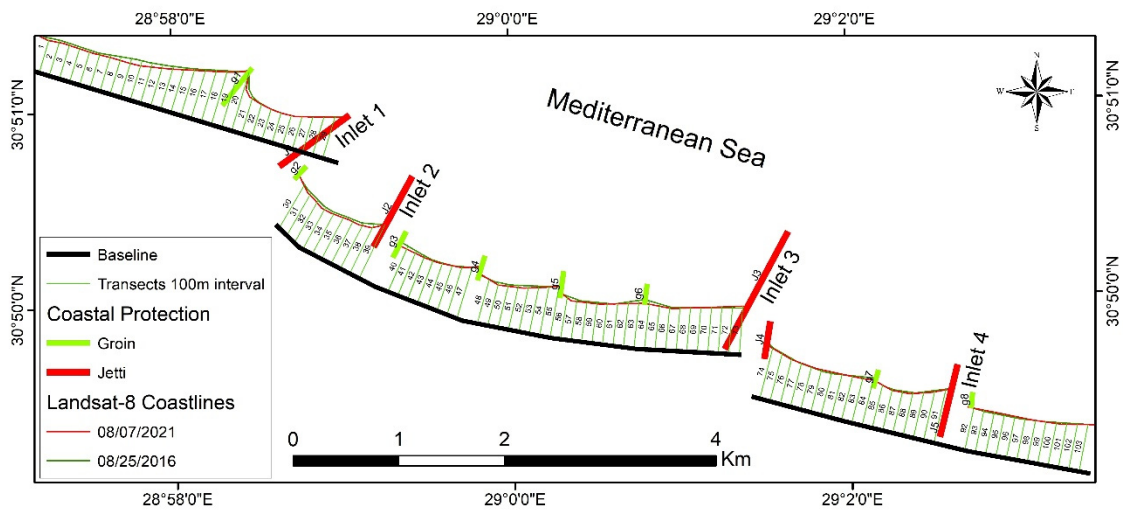


Figure 3. Coastline change analysis using DSAS.

3. Results

Analysis of coastline changes from three different satellites with different spatial resolution for the same time-period from August 2016 to August 2021 indicate that there is difference in net shoreline movement (NSM) and the end point rate along 100 transects with a 100-meter spatial interval, as shown in Figure 4. The summarized results of the shoreline change rate statistics and net shoreline movement are shown in Table 2. In addition, the difference of the highest accretion distance between Landsat-8 and Sentinel-2 reaches 10 m, and between Landsat 8 and PlanetScope it is 6 m. The highest annual rate of coastal erosion and accretion in the study area is nearly ± 2 m/year.

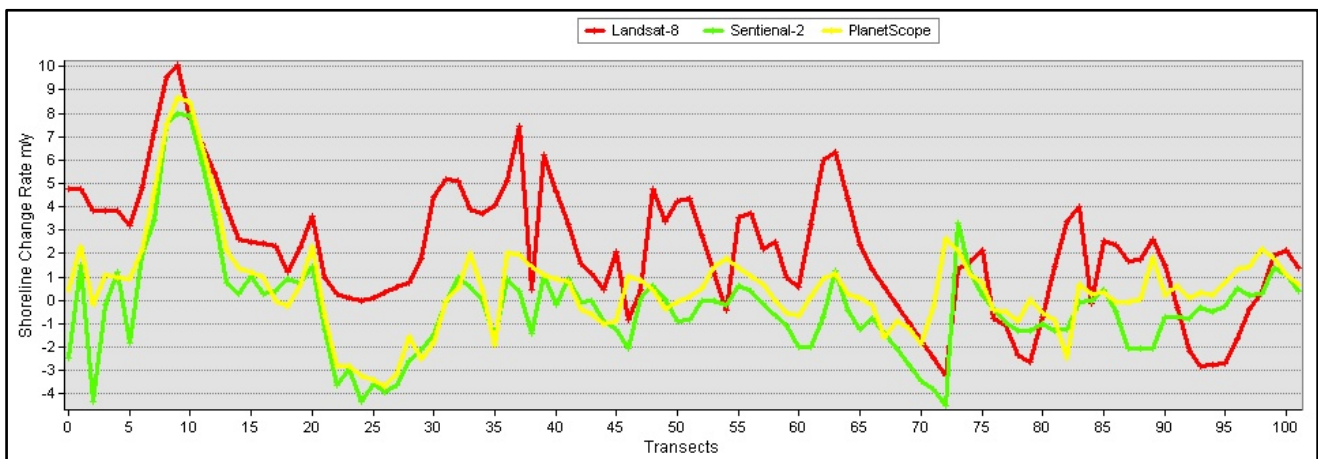


Figure 4. Comparing coastline change rates using different satellite data between 2016 and 2021.

Table 2. Statistics of coastline change difference between 2016 to 2021 in meters.

Parameter	Landsat-8	Sentienel-2	PlanetScope
NSM ¹ Highest Accretion	49.83	39.87	43.84
Highest Erosion	−15.97	−22.44	−18.61
Highest	−3.23	−4.60	−3.69
Erosion Average	−1.50	−1.48	−0.02
Lowest	−0.11	−0.01	−1.19
EPR ² Highest	10.07	8.00	8.70
Accretion Average	3.06	1.50	1.52
Lowest	0.00	0.00	0.01

¹ Net Shoreline Movement (m). ² End Point Rate (m/year).

Spatial variations of the shoreline change rate over the study area refers to a difference of medium and high spatial resolution of satellite data. In transects (1–6), Landsat-8 data give an accretion rate approximately 3 m/year; while Sentinel-2 imagery indicated negative values reaching up to 4 m/year. In addition, large differences in coastline change rates appear in transects 20–30. The shoreline which come from Landsat 8 are higher the negative values from Sentinel-2 data. The transects 90–100 indicated that the shoreline rates from Landsat 8 is lower than PlanetScope and Sentinel-2 rates.

Therefore, the results from this study indicated that the rate of coastal change measured by Sentienel-2 closely tracks those of PlanetScope’s imagery compared to Landsat 8, as shown in Figures 3 and 4. Figure 5 shows the correlation between the shoreline change rates from Landsat-8, Sentinel-2, and PlanetScope. It is clear that there is a strong linear relationship 0.73 between PlanetScope and Sentinel-2 rates; on the other hand, Landsat-8 rates give a weak correlation of 0.30 and 0.38 with PlanetScope and Sentinel-2 rates, respectively.

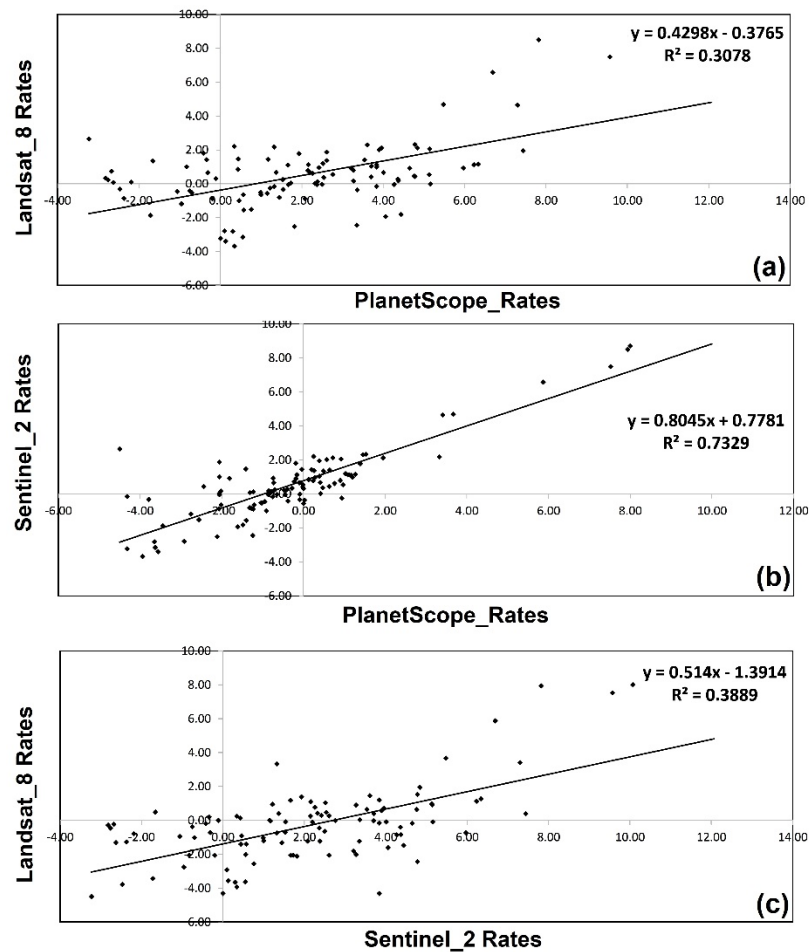


Figure 5. Correlation and linear relationship between different coastline rates. Sub-figure (a) Correlation between Landsat 8 and Sentinel-2 shoreline change rates, sub-figure (b) the correlation between PlanetScope and Sentinel-2 shoreline change, and sub-figure (c) the correlation between Landsat 8 and PlanetScope for shoreline change.

4. Discussion

The analysis of coastlines using three different remote sensing satellites shows that they indicate different rates of coastline change. This is to be expected due to the fact that the satellites have very different footprints. 3 m for PlanetScope, 10 m for Sentinel-2 and 30m for Landsat-8. Coastlines can be extracted and assessed for change more accurately using higher resolution imagery. The accurately of coastline effect on the change detection maps and rate of change. The study area is protected by eight short groins and five jetties to protect the coastline as well as four artificial inlets.

5. Conclusions

This study was the first to compare three different satellites data from medium- to high-resolution imagery to detect and extract linear coastline features as well as change analysis. All of satellite images used in this study can be used for coastline change detection, but some coastline features better identified using higher spatial resolution imagery such as PlanetScope and Sentinel-2A than Landsat-8. Landsat, however, has a much longer history—it was launched in 1972 and therefore is useful for long-term studies of change. Landsat imagery is also free of charge. PlanetScope has the smallest IFOV of the satellites studied (3 m) and therefore is useful when coastline change must be mapped to that level of precision is required. However, it is possible to measure and map coastline

change satisfying many applications using medium resolution imagery from Landsat-8 and Sentinel-2A with are available free of charge.

Author Contributions: Both authors (K.D., S.S.) contributed to all parts equally. All authors have read and agreed to the published version of the manuscript.

Funding: This work has not been supported by any institutions.

Institutional Review Board Statement: Not applicable.

Informed Consent Statement: Not applicable.

Data Availability Statement: Not applicable.

Conflicts of Interest: The authors declare no conflict of interest.

References

1. Yasir, M.; Sheng, H.; Fan, H.; Nazir, S.; Niang, A.J.; Salauddin, M.D.; Khan, S. Automatic Coastline Extraction and Changes Analysis Using Remote Sensing and GIS Technology. *IEEE Access* **2020**, *8*, 180156–180170. [[CrossRef](#)]
2. Kermani, S.; Boutiba, M.; Guendouz, M.; Guettouche, M.S.; Khelfani, D. Detection and analysis of shoreline changes using geospatial tools and automatic computation: Case of jijelian sandy coast (East Algeria). *Ocean Coast. Manag.* **2016**, *132*, 46–58. [[CrossRef](#)]
3. Pardo-Pascual, J.E.; Almonacid-Caballer, J.; Ruiz, L.A.; Palomar-Vázquez, J. Automatic extraction of shorelines from Landsat TM and ETM+ multi-temporal images with subpixel precision. *Remote Sens. Environ.* **2012**, *123*, 1–11. [[CrossRef](#)]
4. Boak, E.H.; Turner, I.L. Shoreline Definition and Detection: A Review. *J. Coast. Res.* **2005**, *21*, 688–703. [[CrossRef](#)]
5. Olmanson, L.; Brezonik, P.; Bauer, M. Remote Sensing for Regional Lake Water Quality Assessment: Capabilities and Limitations of Current and Upcoming Satellite Systems. In *The Handbook of Environmental Chemistry*; Springer: Cham, Switzerland, 2015; Volume 33, pp. 111–140.
6. Milad, N.-J.; Bovolo, F.; Bruzzone, L.; Gege, P. Physics-based Bathymetry and Water Quality Retrieval Using PlanetScope Imagery: Impacts of 2020 COVID-19 Lockdown and 2019 Extreme Flood in the Venice Lagoon. *Remote Sens.* **2020**, *12*, 2381.
7. Cui, B.; Li, X. Coastline change of the Yellow River estuary and its response to the sediment and runoff (1976–2005). *Geomorphology* **2011**, *127*, 32–40. [[CrossRef](#)]
8. Nguyen, U.N.T.; Pham, L.T.H.; Dang, T.D. An automatic water detection approach using Landsat 8 OLI and Google Earth Engine cloud computing to map lakes and reservoirs in New Zealand. *Environ. Monit. Assess.* **2019**, *191*, 235. [[CrossRef](#)]
9. Ansper, A.; Alikas, K. Retrieval of Chlorophyll a from Sentinel-2 MSI Data for the European Union Water Framework Directive Reporting Purposes. *Remote Sens.* **2019**, *11*, 64. [[CrossRef](#)]
10. Planet. Planet Imagery Product Specification. Available online: <https://assets.planet.com/docs/Combined-Imagery-Product-Spec-Dec-2018.pdf> (accessed on 28 September 2021).
11. Gabr, B.; Ahmed, M.; Marmoush, Y. PlanetScope and Landsat 8 Imageries for Bathymetry Mapping. *J. Mar. Sci. Eng.* **2020**, *8*, 143. [[CrossRef](#)]
12. Dewi, R.S.; Bijker, W. Dynamics of shoreline changes in the coastal region of Sayung, Indonesia. *Egypt. J. Remote Sens. Space Sci.* **2020**, *23*, 181–193. [[CrossRef](#)]
13. Darwish, K.; Smith, S.E.; Torab, M.; Monsef, H.; Hussein, O. Geomorphological changes along the Nile Delta coastline between 1945 and 2015 detected using satellite remote sensing and GIS. *J. Coast. Res.* **2017**, *33*, 786–794. [[CrossRef](#)]
14. Astiti, S.; Osawa, T.; Nuarsa, I. Identification Of Shoreline Changes Using Sentinel 2 Imagery Data In Canggü Coastal Area. *ECOTROPIC J. Environ. Sci.* **2019**, *13*, 191–204. [[CrossRef](#)]
15. Kelly, J.T.; Gontz, A.M. Rapid assessment of shoreline changes induced by Tropical Cyclone Oma using CubeSat imagery in southeast Queensland, Australia. *J. Coast. Res.* **2020**, *36*, 72–87. [[CrossRef](#)]
16. Park, S.J.; Achmad, A.R.; Syifa, M.; Lee, C.-W. Machine learning application for coastal area change detection in Gangwon province, South Korea using high-resolution satellite imagery. *J. Coast. Res.* **2019**, *90*, 228–235. [[CrossRef](#)]
17. Mitri, G.; Nader, M.; Abou Dagher, M.; Gebrael, K. Investigating the performance of sentinel-2A and Landsat 8 imagery in mapping shoreline changes. *J. Coast. Conserv.* **2020**, *24*, 40. [[CrossRef](#)]
18. Mansaray, A.S.; Dzialowski, A.R.; Martin, M.E.; Wagner, K.L.; Gholizadeh, H.; Stoodley, S.H. Comparing PlanetScope to Landsat-8 and Sentinel-2 for Sensing Water Quality in Reservoirs in Agricultural Watersheds. *Remote Sens.* **2021**, *13*, 1847. [[CrossRef](#)]
19. Mandanici, E.; Bitelli, G. Preliminary Comparison of Sentinel-2 and Landsat 8 Imagery for a Combined Use. *Remote Sens.* **2016**, *8*, 1014. [[CrossRef](#)]
20. Frihy, O.; Deabes, E. Erosion chain reaction at El-Alamein Resorts on the western Mediterranean coast of Egypt. *Coast. Eng.* **2012**, *69*, 12–18. [[CrossRef](#)]
21. Emam, W.W.M.; Soliman, K.M. Applying geospatial technology in quantifying spatiotemporal shoreline dynamics along Marina El-Alamein Resort, Egypt. *Environ. Monit. Assess.* **2020**, *192*, 459. [[CrossRef](#)]

22. Emam, W.W.M.; Soliman, K.M. Quantitative analysis of shoreline dynamics along the Mediterranean coastal strip of Egypt. Case study: Marina El-Alamein resort. In *Environmental Remote Sensing in Egypt*; Elbeih, S., Negm, A., Kostianoy, A., Eds.; Springer: Cham, Switzerland, 2020.
23. Awad, M.; El-Sayed, H.M. The analysis of shoreline change dynamics and future predictions using automated spatial techniques: Case of El-Omayed on the Mediterranean coast of Egypt. *Ocean Coast. Manag.* **2021**, *205*, 105568. [[CrossRef](#)]
24. McFeeters, S.K. The use of the Normalized Difference Water Index (NDWI) in the delineation of open water features. *Int. J. Remote Sens.* **1996**, *17*, 1425. [[CrossRef](#)]
25. Xu, H. Modification of normalised difference water index (NDWI) to enhance open water features in remotely sensed imagery. *Int. J. Remote Sens.* **2006**, *27*, 3025–3033. [[CrossRef](#)]